Tellus (1981), *33*, 453–462

On spectra and coherence of tropical climate anomalies

By STEFAN HASTENRATH and EDWARD B. KACZMARCZYK, *The University of Wisconsin, Department of Meteorology, Meteorology and Space Science Building, 1225 West Dayton Street, Madison, Wisconsin 53706, U.S.A.*

(Manuscript received October 14, 1980; in final form February 6, 1981)

ABSTRACT

Time series of hydrometeorological indices from key tropical land areas, of sea surface temperature (SST), and of sea level pressure (SLP) for various latitude zones of the Atlantic, as compiled from ship observations, form the major basis for a study of variance and coherence characteristics of tropical circulation and climate. The novel non-integer technique of Schickedanz–Bowen is used.

SLP in the Eastern Equatorial Pacific and SLP and SST in the Atlantic show large variance in the long end of the spectrum, thus reflecting the inertia and trend of atmosphere and hydrosphere. However, a marked preference for SLP variations is apparent around 2.5 years in the Equatorial Atlantic, and around 6 and 20 years in the North Australian region. The behavior of SST in the El Niño region off the Ecuador/Peru coast differs from other parts of the World oceans, in that variance is concentrated at 2–8 and around 15 years, rather than the long end of the spectrum. Variance in regional hydrometeorological series is concentrated around 2–2.5, 10, and 13–21 years. Spatial linkages are most prominent around 2.3, 5, 8, and 14 years, and appear related to preferred modes of circulation and climate anomalies identified by earlier stratification and principal component studies.

1. Introduction

Recent extreme climatic events in various regions of the tropics have focused renewed attention to variations of the large-scale circulation in low latitudes. Couplings of extreme events in distant regions of the tropics have been identified, such as the occasional simultaneity of Northeastern Brazil Sêcas and Ecuador/Peru El Niño (Caviedes, 1973; Hastenrath, 1976; Hastenrath and Heller, 1977; Covey and Hastenrath, 1978); the positive linkage of rainfall in the Central American–Caribbean area with the U.S. Central Great Plains (Hastenrath, 1976); the coherence of rainfall in various areas of the Pacific (Doberitz, 1968); the inverse pressure variations in the Eastern and Western extremities of that great ocean (Walker and Bliss, 1937; Berlage, 1957, 1966; Quinn, 1974; Wyrtki, 1975); and the relation of the South Asian monsoon rainfall to pressure oscillations in the Pacific (Alexander et al., 1974). General circulation mechanisms of regional climate anomalies and their teleconnections have been suggested on the basis of pattern stratification and judicious hypotheses (Bjerknes, 1966, 1969; Quinn, 1974; Hastenrath, 1976, 1978; Hastenrath and Heller, 1977; Covey and Hastenrath, 1978; Lamb, 1978a,b).

Such mechanisms may or may not be operative in a periodic fashion. However, the characteristic time scales of climate and circulation variability, and the preferred frequency bands for spatial coherence have received little attention. The present investigation is intended as a preliminary inventory of spectral characteristics in low latitudes. Objectives are twofold: (a) frequency bands of major variability in the regional climate shall be identified; and (b) the preference for spatial linkage to occur at certain time scales shall be explored. It is expected that such a spectral description may provide insight into the temporal characteristics of general circulation mechanisms.

0040-2826/81/040453-10$02.50/0

2. Spatial coupling of circulation and climate anomalies

The present work is motivated by various earlier studies which have demonstrated teleconnections between extreme events in the climate of certain regions and the concomitant variations of the large-scale circulation. The area considered here extends from the Pacific across the Americas to the Altantic domain. Specific problem complexes identified in earlier studies and of interest here shall be summarized in the following.

(a) *Extreme climatic events in the Central American–Caribbean region*

Drought in the Central American–Caribbean region (Hastenrath, 1976) tends to be associated with an equatorward expansion of the North Atlantic high, and a band of anomalously cold water extending from the coast of West Africa across the North Atlantic; approximately inverse departure configurations being characteristic for abundant rainy seasons. Rainfall in the Central American–Caribbean region is positively correlated with the hydrometeorological conditions in Subsaharan Africa and negatively with precipitation in the U.S. Central Great Plains and sea temperature off the coast of Ecuador and Peru.

(b) *Climatic hazards in Northeast Brazil*

Drought/flood in Northeast Brazil (Hastenrath and Heller, 1977; Hastenrath, 1978; Covey and Hastenrath, 1978) are characterized by anomalously high/low pressure over the South and Equatorial Atlantic, and low/high pressure over the North Atlantic, and a band of anomalously warm/cold water across the North Atlantic. Rainfall in Northeast Brazil is significantly negatively correlated with sea temperature off the West coast of South America.

(c) *Relation of pressure and sea temperature in the North Atlantic*

A negative coupling of sea level pressure anomalies on the equatorward side of the North Atlantic high and sea temperature in a band further South has been found in various stratification studies (Hastenrath, 1976; Hastenrath and Heller, 1977; Lamb, 1978a,b).

(d) *The El Niño phenomenon*

The El Niño phenomenon on the West coast of South America has been explained as an oceanic response to the relaxation of wind stress over the Equatorial Pacific, which in turn is related to the weakening of the Eastern South Pacific high (Quinn, 1974; Wyrtki, 1975; Hurlburt et al., 1976; McCreary, 1976; Barnett, 1977). There is some controversy on whether the abundant rainfall of El Niño is caused or merely accompanied by high sea temperature (Doberitz, 1968). The long-term pressure variations in the Eastern South Pacific tend to run inverse to the pressure over both the Western Pacific and the South Atlantic (Hastenrath and Heller, 1977; Covey and Hastenrath, 1978).

(e) *Large scale pressure oscillations*

Berlage (1957, 1966) defined the "Southern Oscillation" as a pressure see-saw between the North Australian–Indonesian area and the Eastern South Pacific, with a time scale of 1–5 years. A nodal line was found in the South American sector, with pressure variations in the South Atlantic being broadly in phase with the North Australian–Indonesian area, and out of phase with the Eastern South Pacific.

3. Data

The location of time series used in the present study is depicted in Fig. 1. In an effort to investigate the interrelation of large-scale circulation and regional climate, time series of sea level pressure (SLP) and sea surface temperature (SST) in key areas of the tropical Atlantic and Pacific Ocean were chosen for analysis in conjunction with hydrometeorological series representative of selected tropical land areas. The base period used is 1921–72.

The series of hydrometeorological indices for the U.S. Central Great Plains (US), the Central American–Caribbean region (CARIB), the Ecuador/Peru coast (Ec/Peru R), and Northeast Brazil (NE BRAZIL), were constructed from a large number of individual rainfall stations as described earlier (Hastenrath, 1976, 1978; Hastenrath and Heller, 1977; Covey and Hastenrath, 1978). The SST index of the Ecuador/Peru coast (Ec/Peru T) from Hastenrath (1976) allows the illustration of El Niño events and their antitheses.

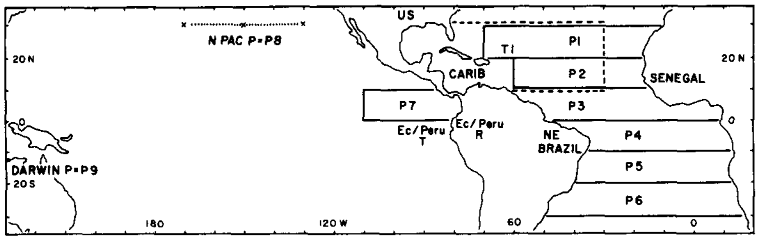

Fig. 1. Orientation map showing location of time series. P and T denote series of sea level pressure (SLP) and sea surface temperature (SST), respectively. Broken-line box refers to T1.

All of the aforementioned indices were constructed as annual values with a compilation by calendar year, except for NE BRAZIL. The latter series is seasonalized for October to September, so as to be centered on the March/April peak of the rainy season (Hastenrath and Heller, 1977). This difference in timing is accounted for in the discussion of phase relationships in Section 6. The discharge of the Senegal river (SENEGAL) provides a similarly useful index for the hydrometeorological conditions over a large tropical region. To this end, individual monthly values were combined by calendar year.

SST and SLP available as monthly means were compiled into annual values by calendar year. A major source for these elements is provided by long-term ship observations in the tropical Atlantic and Eastern Pacific during 1911–72. Details of this data bank have been described by Hastenrath and Lamb (1977). More than 7 million observations were compiled into averages for individual months and one degree square areas. From this data set, time series of SLP and SST were compiled for large ocean blocks (P1–P7, T1). An adequate data coverage results for SLP in the Tropical Atlantic (P1–P6).

For the Pacific, the SLP data by large ocean blocks are deficient and the use of additional sources is desirable. The North Pacific SLP series (P8) represents pressure at the axis of the North Pacific high and had been retrieved from microfilmed Historical Weather Maps, obtained from the National Climate Center, at Asheville, N.C. Darwin provides a long SLP series at a strategic location (P9).

Annual values were used throughout on the following grounds: hydrometeorological index series characterizing the quality of entire rainy seasons are available as annual figures only; a separation into monthly values for the other series would not have substantially improved the time resolution in the frequency bands of interest; and sample calculations with monthly data confirmed the annual results.

4. Methods

Power spectra were calculated by means of an Illinois State Water Survey program (Schickedanz and Bowen, 1977; Hastenrath and Wendland, 1979). This innovative technique produces spectral estimates for equal increments of wavelength by utilizing non-integer values in the sine and cosine waveforms. This procedure is particularly suited to identify periodicities in relatively short data records. "Normalized spectral density" has the conventional meaning only at integer multiples of the fundamental frequency. Schickedanz and Bowen also developed a method for the determination fo *a priori* significance levels. This is here used only for selecting prominent frequencies, rather than for assessing confidence levels as such. Inasmuch as the timing of extrema is obtained for each frequency, phase relationships between series can also be examined. The time of the first maximum falling within the observation period is used here to describe the phase.

In addition, a BMD–02T computer program (Dixon, 1973) was converted to produce a Blackman–Tukey style power spectrum and a Hamon–Hannan type cross spectrum analysis (Blackman and Tukey, 1958; Goodman et al., 1961; Hamon and Hannan, 1963; World Meteorological Organization, 1966; Panofsky and Brier, 1968; Doberitz, 1968, 1969). Results confirm the Schickedanz–Bowen analysis, but are not presented here.

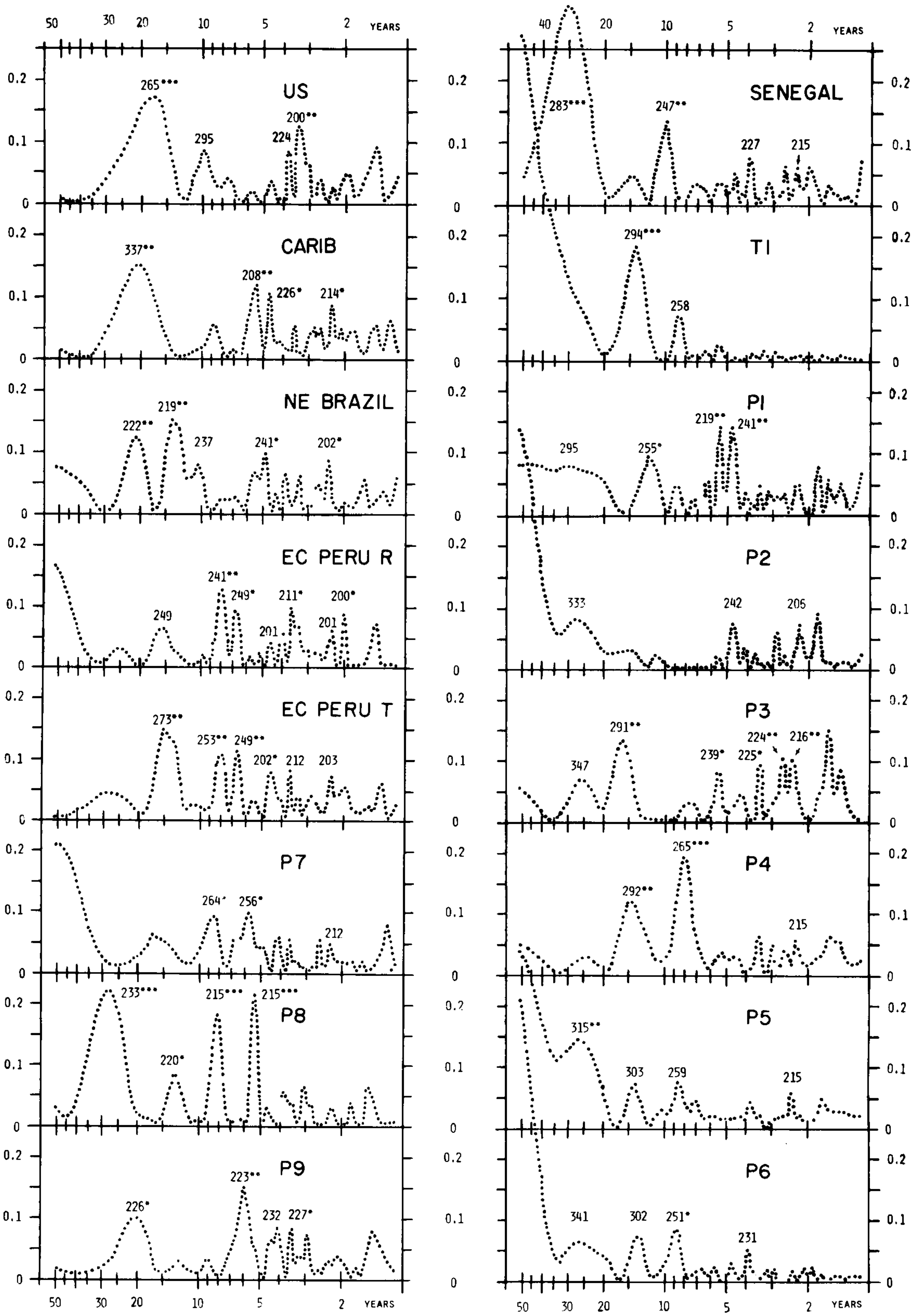
50 30 20 10 5 2 YEARS
0.2
0.1
0
US
265***
295
224
200**
CARIB
337**
208**
226*
214*
NE BRAZIL
222**
219**
237
241*
202*
EC PERU R
249
241**
249*
201
211*
201
200*
EC PERU T
273**
253**
249**
202*
212
203
P7
264*
256*
212
P8
233***
220*
215***
215***
P9
226*
223**
232
227*
SENEGAL
283***
247**
227
215
TI
294***
258
PI
295
255*
219**
241**
P2
333
242
206
P3
347
291**
239*
225*
224**
216**
P4
292**
265***
215
P5
315**
303
259
215
P6
341
302
251*
231
40

5. Power spectra

Fig. 2 shows the power spectra obtained from the Schickedanz–Bowen technique with a time resolution of 0.1 years. Climatic variability and spatial couplings at the scale of 10–25 years merits particular attention, but it is realized that the low frequencies are poorly sampled because of the limited length of climatological records.

SLP shows large variance in the long end of the spectrum over most of the tropical Atlantic (especially P2, P5, P6), the Eastern Equatorial (P7) and the North Pacific (P8). This bears out the tendency for persistence of large-scale pressure patterns. By contrast, a marked preference for frequencies around 2.5 years is apparent in the Equatorial Atlantic (P3), while in the North Australian (P9) region SLP variance is concentrated around 3–7 and 20 years. Spectral power around 5 years is also comparatively important on the equatorward side of the North Atlantic high (P1, P2). The maximum spectral power in the 3–7 year frequency band at Darwin (P9) compares with Berlage's (1966) concept of the "Southern Oscillation" as a pressure variation with a periodicity of 1–5 years. The quasi-biennial SLP fluctuation in the Equatorial Atlantic is of interest in large-scale couplings to be discussed in Sections 6 and 7.

Strong persistence in SST of the North Atlantic (T1) reflects the inertia and trend of the hydrosphere. However, a distinctly different spectrum is characteristic of SST along the Ecuador/Peru coast (Ec/Peru T), in that variance is concentrated at 2–8 and around 15 years. Preference for similar frequencies is also apparent for the rainfall in the coastal zone (Ec/Peru R). In fact, the alternation of El Niño and counter-El Niño events distinguishes the West coast of South America from the SST variance in other parts of the World oceans.

By comparison with oceanic SLP and SST, persistence seems of lesser importance for the hydrometeorological conditions of the tropical land areas. Rainfall in the Central American–Caribbean region (CARIB) varies with preference at the time scales of 2–2.5, 5, and 20 years. The variance of rainfall in the U.S. Central Great Plains (US) is concentrated around 3–4 and 10–17 years. The water discharge of Senegal river (SENEGAL) shows a preference for variations around 2–4, 10, and 30 years. Rainfall in Northeast Brazil (NE BRAZIL) shows comparatively large variance around 2.5, 5, 10, and 13–21 years. This is broadly consistent with the results of Markham (1974).

A quasi-biennial oscillation thus prevails in equatorial Atlantic SLP (P3, P4) and in the hydrometeorological conditions of neighboring continental regions (NE BRAZIL, CARIB, SENEGAL). This pulse is also apparent in SST along the South American West Coast (Ec/Peru T). The 3–7-year frequency band is conspicuous in SLP in the North Australian region (P9) and on the equatorward side of the North Atlantic high (P1, P2), as well as in some hydrometeorological index series (NE BRAZIL, CARIB). Persistence is particularly dominant in South Atlantic SLP (P5, P6) and North Atlantic SST (T1).

6. Spatial couplings

(a) *Correlation coefficients*

A first orientation on spatial linkages is obtained from Table 1. In estimating the significance of correlation coefficients, Quenouille's (1952, p. 168) method was used to account for the reduction of effective degrees of freedom due to persistence.

As can be expected, there is a high correlation between SLP in neighboring regions of the Atlantic. More interesting is an inspection of Table 1 in terms of the five problem complexes reviewed in Section 2.

Rainfall in the Central American–Caribbean region (CARIB) is indeed negatively correlated with SLP in the North Atlantic (P1, P2, P3), rainfall in the U.S. Central Great Plains (US), and SST off Ecuador and Peru (Ec/Peru T); and positively with the discharge of the Senegal river (SENEGAL). There is also a high negative correlation with SLP in the North Australian region (P9).

Consistent with earlier studies, rainfall in Northeast Brazil (NE BRAZIL) is negatively correlated with SLP over the South Atlantic (P4, P5, P6), and SST off Ecuador and Peru (Ec/Peru T). The negative linkage between SLP on the equatorward side of the North Atlantic high (P1) and SST in a

Fig. 2. Power spectra of time series indicated in Fig. 1. Normalized spectral densities (vertical scale) are entered as dotted lines, one, two, and three asterisks indicating three arbitrary thresholds. Numbers ascribed to the respective peaks signify the date of the first maximum in tenths of years (i.e. 217 = 1921.7).

Table 1. *Correlation coefficients between time series shown in the orientation map Fig. 1, in hundredths. One, two, three, and four dots under the number denote statistical significance at the 10, 5, 1, and 0.1 percent levels, respectively. See Fig. 1 for location of time series*

	P1	P2	P3	P4	P5	P6	P7	P8	P9	T1	CARIB	US	SENE-GAL	NE BRAZIL	Ec/Peru T	Ec/Peru R
P1		+67 ••••	+23 •	+10	+33 ••	+26 •	+13	−3	−11	−26 •	−16	−7	+15	+11	−10	−3
P2			+49 ••••	+31 ••	+59 ••••	+64 ••••	+29 ••	−29 •	−6	+24	−27 ••	−8	+11	−11	+9	−17
P3				+73 ••••	+60 ••••	+41 ••••	−5	−32 ••	+28 ••	+26 •	−45 ••••	+6	+4	−20	+21	−2
P4					+72 ••••	+52 ••••	+14	−32 ••	+9	+36 •••	−16	+4	+1	−34 ••	+31 ••	−5
P5						+83 ••••	+19	−26	−1	+31 •	−6	−8	+10	−32 ••	+13	−17
P6							+43 ••••	−30 •	−15	+50 ••••	−2	−2	+7	−27	+8	−30
P7								+9	−56 ••••	+30 ••	+30 •	−11	+4	+7	−39 ••••	−59 ••••
P8									−35 ••	−27 •	+24 ••	−26 •	+8	+7	−24 •	+10
P9										+3	−45 ••••	+31 ••	−32 ••	−1	+42 ••••	+23
T1											−14	+17	−30 •	−40 ••••	+24 •	−35 ••
CARIB												−41 ••••	+34 ••	−16	−43 •••	−25
US													−21	−3	+24	+1
SENEGAL														+17	−41 ••••	+0
NE BRAZIL															−34 ••	−1
Ec/Peru T																+50 ••••
Ec/Peru R																

band further South (T1) is also apparent from Table 1.

SST off the coast of Ecuador and Peru is the key parameter with regard to the El Niño phenomenon and its antithesis. In fact, this parameter (Ec/Peru T) is positively correlated with SLP over the South Atlantic (P4, P5, P6) and in the North Australian region (P9), and negatively with SLP over the Eastern Pacific (P7). The correlation is of course positive with rainfall along the Ecuador–Peru coast (Ec/Peru R), but negative with rainfall in the Central American–Caribbean region (CARIB) and in Northeast Brazil (NE BRAZIL). Large-scale pressure oscillations are further reflected in Table 1 by SLP in the North Australian region (P9) being negatively correlated with the Eastern Pacific (P7).

The large-scale couplings shall be examined in the following by ways of maps for various frequency bands (Fig. 3), for which a marked preference is revealed in Fig. 2.

(b) *The 2.2–2.4-year frequency band*

Fig. 3a for this frequency band illustrates a multitude of large-scale spatial couplings, relating in particular to the extreme hydrometeorological events in the Central American–Caribbean region and Northeast Brazil, and the El Niño phenomenon as reviewed in Sections 2a, b, and d.

Rainfall variations in the Central American–Caribbean region (CARIB) run approximately parallel to the water discharge of the Senegal river (SENEGAL), and inverse to SLP on the equatorward side of the North Atlantic high (P2, P3), and SST at the Ecuador–Peru coast (Ec/Peru T). The minimum of Central American–Caribbean rainfall (CARIB) approximately coincides with the concurrent maxima of SST and rainfall at the Ecuador–Peru coast (Ec/Peru T, Ec/Peru R).

Of interest with regard to the El Niño phenomenon is the fact that the maximum of SST off the Ecuador–Peru coast (Ec/Peru T) follows both the minimum of SLP over the Eastern Pacific (P7) and the maximum in coastal rainfall (Ec/Peru R). A similar phase lag between rainfall and SST anomaly has been suggested by Doberitz (1968). It appears that both anomalies may be in response to changes in the atmospheric circulation, although a warm ocean may provide a secondary enhancement of rainfall activity.

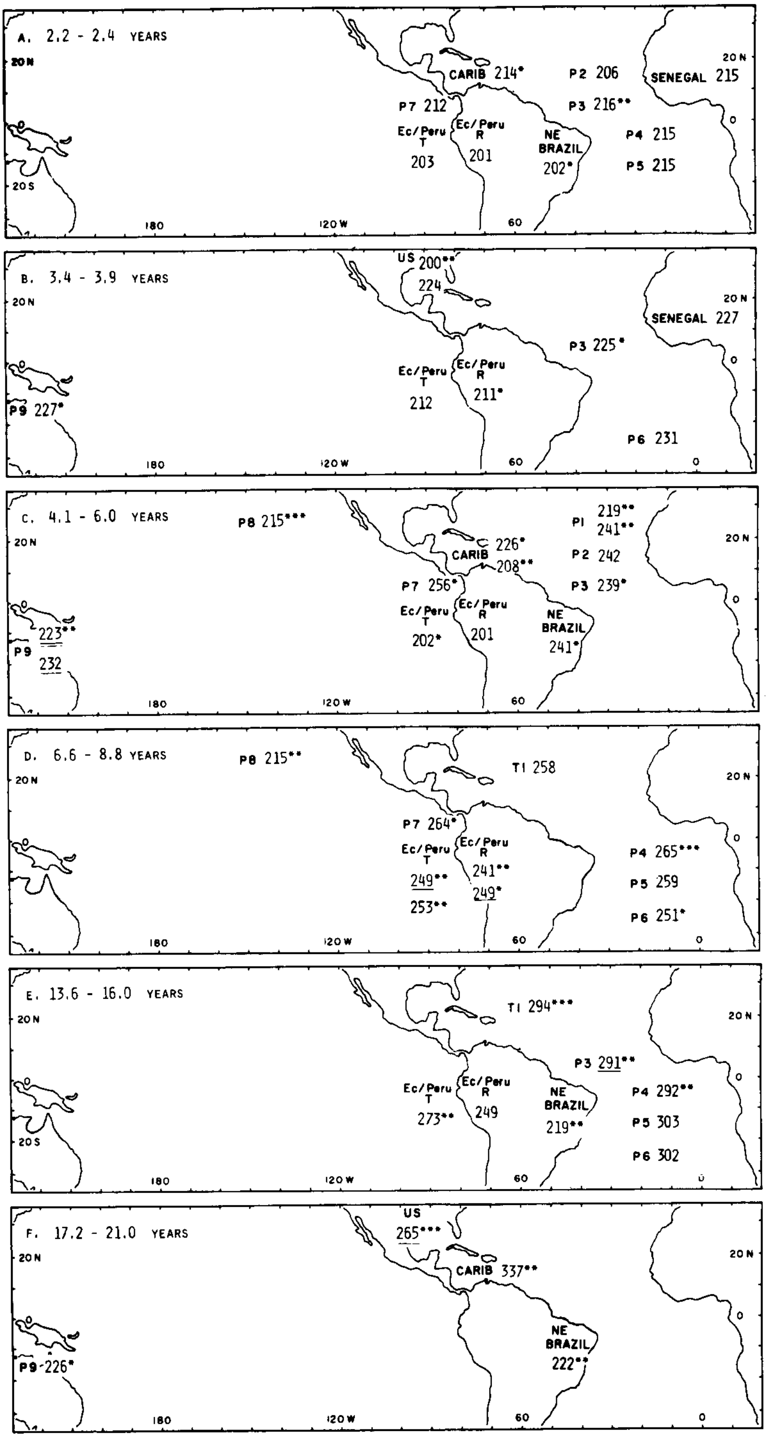

Fig. 3. Phase relationships at preferred frequencies: a. 2.2, 2.3, and 2.4 years; b. 3.4, 3.5, 3.6, 3.8, and 3.9 years; c. 4.1, 4.7, 4.9, 5.4, 5.5, 5.8, and 6.0 years, the 4.1 and 6.0 year frequencies being identified by single and double underlining; d. 6.6, 6.7, 7.9, 8.0, 8.2, and 8.8 years, the 6.6 and 6.7 year frequencies being identified by underlining; e. 13.6, 14.0, 14.7, 14.8 and 16.0 years, the 16.0 year frequency being identified by underlining. f. 17.2, 20.5, 21.0 years, the 17.2 frequency being identified by underlining. Numbers indicate date of maximum in tenths of years (i.e. 217 = 1921.7). Asterisks have same meaning as in Fig. 2.

Consistent with the discussion in Section 2b, the minimum of rainfall in Northeast Brazil (NE BRAZIL) is approximately synchronous with the maximum of SLP in the South Atlantic (P4, P5). SLP in neighboring bands of the equatorial Atlantic (P3, P4, P5) is in phase.

(c) *The 3.4–3.9-year frequency band*

Reference is made to Fig. 3b. Broadly consistent with the discussion in Sections 2d and e, the concurrent maxima of SST and rainfall at the Ecuador–Peru coast (Ec/Peru T, Ec/Peru R) are approximately synchronous with the minima of SLP in the equatorial (P3) and South Atlantic (P6) and in the North Australian region (P9).

(d) *The 4.1–6.0-year frequency band*

In this frequency band (Fig. 3c), the linkages with SLP in the North Australian region (P9) are particularly conspicuous. Consistent with the discussion in Sections 2d and e, the maximum of SLP at Darwin (P9) is approximately synchronous with the minimum of SLP in the Eastern Pacific (P7).

(e) *The 6.6–8.8-year frequency band*

In this frequency band (Fig. 3d) variations of SST and rainfall at the Ecuador–Peru coast (Ec/Peru T, Ec/Peru R) are essentially synchronous, and in phase with SLP in the South Atlantic (P4, P5, P6). This agrees largely with the review in Sections 2a, d, and e. SLP in neighboring bands of the Atlantic (P4, P5, P6) is approximately in phase.

(f) *The 13.6–16.0-year frequency band*

This frequency band (Fig. 3e) is particularly interesting in regard to linkages with the hydrometeorological conditions in Northeast Brazil. Northeast Brazil rainfall (NE BRAZIL) has a march broadly inverse to that of SLP over the South and equatorial Atlantic (P4, P5, P6). Variations of SST off the Ecuador–Peru coast (Ec/Peru T) are approximately synchronous with those of SLP over the South and equatorial Atlantic (P4, P5, P6), and with the rainfall variations at the Ecuador–Peru littoral (Ec/Peru R), the latter leading slightly. The aforementioned spatial couplings in Fig. 3e are related to the review in Sections 2b, d, e, in particular.

(g) *The 17.2–21.0-year frequency band*

Results are mapped in Fig. 3f. At this time scale, rainfall in the Central American–Caribbean region (CARIB) runs approximately inverse to that in the Central U.S. Great Plains (US), and in Northeast Brazil (NE BRAZIL). The spatial linkage indicated in Fig. 3f is consistent with the discussion in Sections 2a, b.

7. Summary and conclusions

A series of earlier studies have demonstrated the interrelation of regional climate anomalies and variations in the large-scale circulation. Motivated by these investigations, an attempt was made in the present study to compile a preliminary inventory of the preferred frequency bands of climatic variability, and to explore the time scales at which spatial linkages occur with preference.

Climatic variability (Fig. 2) is concentrated in different frequency bands for the various regions. Rainfall in the Central American–Caribbean region (CARIB) shows a preference for variations at the time scale of 2–2.5, 5 and 20 years. The negatively correlated (Table 1) rainfall in the U.S. Central Great Plains (US), however, varies with preference around 3–4 and 10–17 years. The water discharge of the Senegal River (SENEGAL), which is positively correlated (Table 1) with the hydrometeorological conditions in the Central American–Caribbean domain (CARIB), has variance concentrated around 2–4, 10 and 30 years. Rainfall in Northeast Brazil (NE BRAZIL) shows a preference for variations around 2.5, 5, 10 and 13–21 years.

SLP in the Atlantic (especially P2, P5, P6) and Eastern Equatorial Pacific (P7), and SST in a portion of the North Atlantic (T1) shows large variance in the long end of the spectrum, thus reflecting the inertia and trend of atmosphere and hydrosphere. This contrasts with the spectrum of SST in the El Niño region off the West Coast of South America (Ec/Peru SST), where variance is concentrated around 2–8 and 15 years. Furthermore, there is a marked preference for SLP variations around 2.5 years in the Equatorial Atlantic (P3, P4), and around 3–7 and 20 years in the North Australian region (P9).

Spatial linkages (Fig. 3) are most pronounced around 2.2–2.4, 4.7–5.5, 7.9–8.8, and 13.6–14.7

years. A variety of spatial couplings relate to the hydrometeorological conditions in the Central American–Caribbean region (CARIB). The negative correlation (Table 1) with rainfall in the U.S. Central Great Plains (US) results mostly from frequencies around 20 years. The inverse linkage (Table 1) with SST off Ecuador/Peru (Ec/Peru SST) occurs in part near 2.3 years.

Rainfall in Northeast Brazil (NE BRAZIL) is coupled with SLP over the South Atlantic (P4, P5, P6) at 13.6–14.7 years. The negative linkage (Table 1) with SST off the West Coast of South America (Ec/Peru SST) is concentrated around 2.5 years.

SST off Ecuador–Peru (Ec/Peru SST) is linked negatively with SLP over the Eastern Equatorial Pacific (P7) at 2.3 years. The positive correlation (Table 1) with SLP over the Equatorial Atlantic (P3, P4) and the North Australian region (P9) appears to result from contributions at a variety of frequencies. The large-scale SLP oscillations, in which the Western Pacific (P9) tends to run inverse to the Eastern Pacific (P7), are concentrated around 6 years.

Characteristic departure patterns in atmospheric and hydrospheric fields, as reviewed in Section 2, were identified by stratification. This effort was complemented by principal component analysis for the period 1948–72 (Hastenrath, 1978). Time series of principal components, representing preferred modes of circulation and climate anomalies, were also subjected to spectral analysis. Results not detailed here support the discussion for the larger time scales in Sections 6f and g but the compact principal component representation of time series ensembles and the use of different base periods pose serious limitations.

Geophysical time series are commonly nonstationary. Accordingly, the present exploratory study does not provide more than a spectral description of regional climate variability and large-scale couplings representative of the observation period analyzed; identification of preferred time scales being of primary interest. As such, it may serve as background for investigations into the mechanisms of climate and circulation anomalies.

8. Acknowledgements

This study was supported by the NSF Climate Dynamics Research Program. We thank J. Kutzbach, T. Starr, and E. Wahl for comments on draft versions of this paper.

REFERENCES

Alexander, G., Keshavamurty, R. N., Mikhopadhyay, R. K. Bhosale, S. G. 1974. Pacific equatorial pressure gradient and Indian monsoon rainfall. *Nature 252*, 463–464.

Barnett, T. P. 1977. An attempt to verify some theories of El Niño. *J. Phys. Oceanogr. 7*, 633–647.

Berlage, H. P. 1957. *Fluctuations of the general circulation of more than one year, their nature and prognostic value.* Koninklijk Nederlands Meteorologisch Instituut, Mededelingen en Verhandelingen, No. 69, 152 pp.

Berlage, H. P. 1966. *The Southern Oscillation and world weather.* Koninklijk Nederlands Meteorologisch Instituut, Mededelingen en Verhandelingen, No. 88, 152 pp.

Bjerknes, J. 1966. A possible response of the atmospheric Hadley circulation to equatorial anomalies of ocean temperature. *Tellus 18*, 820–829.

Bjerknes, J. 1969. Atmospheric teleconnections from the equatorial Pacific. *Mon. Wea. Rev. 97*, 163–172.

Blackman, R. B. and Tukey, J. W. 1958. *The measurement of power spectra.* New York: Dover Publications, Inc., 190 pp.

Caviedes, C. N. 1973. Sêcas and El Niño: two simultaneous climatical hazards in South America. *Proc. Assoc. Amer. Geogr. 5*, 44–49.

Covey, D. L. and Hastenrath, S. 1978. The Pacific El Niño phenomenon and the Atlantic Circulation. *Mon. Wea. Rev. 106*, 1280–1287.

Dixon, W. J. ed. 1973: Autocovariance and power spectrum analysis. In *Biomedical computer programs.* Los Angeles: University of California Press, 517–540.

Doberitz, R. 1968. Cross spectrum analysis of rainfall and sea temperature at the Equatorial Pacific Ocean. *Bonner Meteorol. Abhandlungen 8*, 55 pp.

Doberitz, R. 1969. Cross spectrum and filter analysis of monthly rainfall and wind data in the tropical Atlantic region. *Bonner Meteorol. Abhandlungen 11*, 53 pp.

Goodman, N. R., Katz, S., Kramer, B. H. and Kuo, M. T. 1961. Frequency response from stationary noise: two case histories. *Technometrics 3*, 245–268.

Hamon, B. V. and Hannan, E. J. 1963. Estimating relations between time series. *J. Geophys. Res. 68*, 6033–6041.

Hastenrath, S. 1976. Variations in low-latitude circulation and extreme climatic events in the tropical Americas. *J. Atm. Sci. 33*, 202–215.

Hastenrath, S. 1978. On modes of tropical circulation and climate anomalies. *J. Atm. Sci. 35*, 2222–2231.

Hastenrath, S. and Heller, L. 1977. Dynamics of climatic hazards in northeast Brazil. *Quart. J. Roy. Meteorol. Soc. 103*, 77–92.

Hastenrath, S., Lamb, P. 1977. *Climatic atlas of the tropical Atlantic and Eastern Pacific Oceans*. University of Wisconsin Press.

Hastenrath, S. and Wendland, W. M. 1979. On the secular variation of storms in the tropical North Atlantic and Eastern Pacific. *Tellus 31*, 28–38.

Hurlburt, H., Kindle, J. and O'Brien, J. 1976. A numerical simulation of the onset of El Niño. *J. Phys. Oceanogr. 6*, 632–645.

Kidson, J. W. 1975. Tropical eigenvector analysis and the Southern Oscillation. *Mon. Wea. Rev. 103*, 187–196.

Lamb, P. 1978a. Case studies of tropical Atlantic surface circulation patterns during recent Sub-Saharan weather anomalies. *Mon. Wea. Rev. 106*, 482–491.

Lamb, P. 1978b. Large-scale tropical Atlantic surface circulation patterns associated with Subsaharan weather anomalies. *Tellus 30*, 240–251.

Markham, C. G. 1974. Apparent periodicities in rainfall at Fortaleza, Ceará, Brazil. *J. Appl. Meteorol. 13*, 176–179.

McCreary, J. 1976. Eastern tropical ocean response to changing wind systems; with application to El Niño. *J. Phys. Oceanogr. 6*, 632–645.

Panofsky, H. A. and Brier, G. W. 1968. *Some applications of statistics to meteorology*. Pennsylvania State University Press, 224 pp.

Quenouille, M. H. 1952. *Associated measurements*. London: Butterworths Scientific Publications, 242 pp.

Quinn, W. H. 1974. Monitoring and predicting El Niño invasions. *J. Appl. Meteorol. 13*, 825–830.

Schickedanz, P. T. and Bowen, E. G. 1977. The computation of climatological power spectra. *J. Appl. Meteorol. 16*, 359–367.

Walker, G. T. and Bliss, C. W. 1937. World weather, VI. *Mem. Roy. Meteorol. Soc. Vol. 4*, No. 39, 119–139.

World Meteorological Organization, 1966. *Climatic change*. WMO Technical Note No. 79, Geneva,, 79 pp.

Wyrtki, K. 1975. El Niño—the dynamic response of the Equatorial Pacific Ocean to atmospheric forcing. *J. Phys. Oceanogr. 5*, 572–584.

О СПЕКТРАХ И КОГЕРЕНТНОСТИ ТРОПИЧЕСКИХ АНОМАЛИЙ КЛИМАТА

Временные ряды гидрометеорологических индексов для ключевых тропических областей суши, ряды данных по температуре морской поверхности (ТМП) и по давлению на уровне моря (ДУМ) для различных широтных зон в Атлантике, собранные по корабельным наблюдениям, образуют хорошую основу для изучения характеристик изменчивости и когерентности циркуляции и климата в тропиках. Используется новая нецелая техника Шикеданца-Боуэна.

Величины ДУМ в восточной экваториальной части Тихого океана и ДУМ и ТМП в Атлантике имеют большую изменчивость в длиннопериодном конце спектра, отражая таким образом инерцию и тренды в атмосфере и гидросфере. Однако заметная предпочтительность для вариаций ДУМ имеется вблизи 2.5 лет в экваториальной Атлантике в вблизи 6 и 20 лет в области северной Австралии. Поведение ТМП в области Эль-Ниньо вне берегов Эквадора и Перу отличается от такового в других частях Мирового океана тем, что изменчивость сконцентрирована при 2–8 и вблизи 15 лет, а не в длиннопериодном конце спектра. Изменчивость в региональных гидрометеорологических рядах концентрируется вблизи 2–2.5, 10 и 13–21 года. Пространственные связи наиболее заметны вблизи 2.3, 5, 8 и 14 лет и представляются связанными с предпочтительными модами циркуляции и климатических аномалий, идентифицированных предыдущими исследованиями стратификации и главных компонент.